Optics Communications 380 (2016) 79–86

Contents lists available at ScienceDirect

Optics Communications

journal homepage: www.elsevier.com/locate/optcom

Scintillation index of Gaussian waves in weak turbulent ocean

Zhiqiang Wang [a,b], Pengfei Zhang [a], Chunhong Qiao [a], Lu Lu [a,b,*], Chengyu Fan [a,**], Xiaoling Ji [c,**]

[a] Key Laboratory of Atmospheric Composition and Optical Radiation, Anhui Institute of Optics and Fine Mechanics, Chinese Academy of Sciences, Hefei 230031, China
[b] University of Science and Technology of China, Hefei 230026, China
[c] Department of Physics, Sichuan Normal University, Chengdu 610066, China

ARTICLE INFO

Article history:
Received 7 April 2016
Received in revised form
17 May 2016
Accepted 31 May 2016
Available online 6 June 2016

Keywords:
Scintillation index
Gaussian wave
Oceanic turbulence

ABSTRACT

The analytical expressions of radial and the longitudinal components of scintillation index are derived in weak oceanic turbulence. The effects of off-axis distance, propagation distance, and three oceanic parameters (i.e., the ratio of temperature to salinity contribution to the refractive index spectrum w, the rate of dissipation of the mean squared temperature χ_T and the rate of dissipation of the turbulent kinetic energy ε) on radial component of scintillation index are examined. The influences of propagation distance and three oceanic parameters on the longitudinal component of scintillation index are investigated. It is shown that the radial component of scintillation increases as off-axis distance increases. Both radial and longitudinal components of scintillation increase as propagation distance, w and χ_T increase while decreases as ε increases. Besides, the longitudinal component of scintillation increases more drastically for plane wave than others, which indicates the plane wave is affected the most at the fixed turbulent strength. The longest weak turbulence distance for a plane wave is shorter than that for a Gaussian or spherical wave.

1. Introduction

Knowledge of the scintillation index is crucial for determining system performance in laser communication system or laser radar link [1]. The scintillation is detrimental to the performance of free-space optical (FSO) communication systems because it degrades the signal-to-noise ratio (SNR) and increases the bit error rate (BER). Investigation of scintillation of laser beams in a turbulent atmosphere become more and more important because of their wide applications in FSO communications and imaging systems [2]. Within the last few years, some studies have been reported on the scintillations in weak [3–15] and strong [16,17] atmospheric turbulence. Until now, scintillation of laser beam in oceanic turbulence is relatively less explored compared to that in atmospheric turbulence. It is clear that the propagation of optical beams in underwater channels will cause fluctuations in the intensity measured by the scintillation index, which is an important criterion of the performance of communication. Hence, an understanding of scintillation is imperative in seawater. Since 1978, it is known that oceanic turbulence, which is induced by temperature and salinity fluctuations, is measured separately and developed analytically [18]. Recently, the scintillations for plane and spherical waves propagating through oceanic turbulence with emphasis on the contribution from salinity-induced turbulence have been reported [19]. The longitudinal components of scintillations of optical plane and spherical waves in underwater turbulence have been investigated numerically [20]. Propagation behavior of scintillation index and bit error rate of a partially coherent flat-topped laser beam in oceanic turbulence have been reported [21]. Baykal has researched intensity fluctuations of multimode laser beams in underwater medium [22], higher-order laser beam scintillation in oceanic medium [23] and weakly turbulent marine atmospheric medium [24], and scintillation index in strong oceanic turbulence [25]. However, the analytical expressions of scintillation index have never been reported. In this paper, based on the Rytov method, we deduce the analytical formulae of the radial and longitudinal components of scintillation index for a general Gaussian-beam wave propagating through oceanic turbulence. The influences of the off-axis distance, propagation distance, and three oceanic parameters (i.e., the ratio of temperature to salinity contribution to the refractive index spectrum w, the rate of dissipation of the mean squared temperature χ_T and the rate of dissipation of the

* Corresponding author at: Key Laboratory of Atmospheric Composition and Optical Radiation, Anhui Institute of Optics and Fine Mechanics, Chinese Academy of Sciences, Hefei 230031, China.
** Corresponding authors.
E-mail addresses: luquanchengll@sina.com (L. Lu), cyfan@aiofm.ac.cn (C. Fan), jixl100@163.com (X. Ji).

http://dx.doi.org/10.1016/j.optcom.2016.05.089
0030-4018/

turbulent kinetic energy ε) on underwater scintillations are investigated.

2. Scintillation index of Gaussian wave

We assume that seawater is homogeneous and isotropic when the eddy thermal diffusivity and the diffusion of salt are assumed to be equal, the power spectrum is given by [26,27]

$$\Phi_n(\kappa) = 0.388\times10^{-8}\varepsilon^{-1/3}\kappa^{-11/3}[1+2.35(\kappa\eta)^{2/3}]\frac{\chi_T}{w^2}(w^2e^{-A_T\delta} + e^{-A_S\delta} - 2we^{-A_{TS}\delta}), \tag{1}$$

where $A_T = 1.863\times10^{-2}$, $A_S = 1.9\times10^{-4}$, $A_{TS} = 9.41\times10^{-3}$, $\delta = 8.284(\kappa\eta)^{4/3} + 12.978(\kappa\eta)^2$. η is the Kolmogorov micro scale (inner scale), ε is the rate of dissipation of kinetic energy per unit mass of fluid ranging from 10^{-1} m^2/s^3 to 10^{-10} m^2/s^3, χ_T is the rate of dissipation of mean-squared temperature and has the range 10^{-4} K^2/s to 10^{-10} K^2/s [27]. Additionally, w (unitless) defines the ratio of temperature and salinity contributions to the refractive index spectrum, which in the ocean waters can vary in the interval $[-5; 0]$, with -5 and 0 corresponding to dominating temperature-induced and salinity-induced optical turbulence, respectively [27].

Under the assumption of weakly turbulent fluctuations the scintillation index of a Gaussian beam can be represented by the sum of the radial component and the longitudinal (on-axis) component, i.e. [28]

$$\sigma_I^2(\mathbf{r}, L) = \sigma_{I,r}^2(\mathbf{r}, L) + \sigma_{I,l}^2(L), \tag{2}$$

where

$$\sigma_{I,r}^2(\mathbf{r}, L) = 8\pi^2k^2L\int_0^1\int_0^\infty \kappa\Phi_n(\kappa)\exp(-\Lambda L\kappa^2\xi^2/k)\left[I_0(2\Lambda r\xi\kappa) - 1\right]d\kappa d\xi, \tag{3}$$

$$\sigma_{I,l}^2(L) = 8\pi^2k^2L\int_0^1\int_0^\infty \kappa\Phi_n(\kappa)\exp(-\Lambda L\kappa^2\xi^2/k)\left\{1 - \cos\left[L\kappa^2\xi(1-\bar{\Theta}\xi)/k\right]\right\}d\kappa d\xi, \tag{4}$$

here $I_0(\bullet)$ is the modified Bessel function of order zero, and Λ and $\bar{\Theta}$ are the normalized parameters of the Gaussian beam [28].

On substituting from Eq. (1) into (Eqs. (3)–4), one can determine the scintillation index of a Gaussian beam propagating through the ocean. The radial component of the scintillation index (see Appendix in this paper) leads to

$$\sigma_{I,r}^2(\mathbf{r}, L) \approx 1.949\Lambda^2r^2W^2L\varepsilon^{-1/3}\frac{\chi_T}{w^2}[(3.641\times10^{-6}w^2 - 2.323\times10^{-6}w + 6.728\times10^{-6})k^2W^2 - (w^2 - 5.421w + 770.381)L^2], \tag{5}$$

In the special cases of plane wave ($\Lambda = 0$, $\bar{\Theta} = 0$) and spherical wave ($\Lambda = 0$, $\bar{\Theta} = 1$) the radial component of the scintillation index vanishes.

The corresponding expression for the longitudinal component of the scintillation index is

$$\sigma_{I,l}^2(L) \approx 0.388\times10^{-8}\pi^2\varepsilon^{-1/3}\frac{\chi_T}{w^2}\Bigg[4L^3\left(\frac{1}{3} - \frac{\bar{\Theta}}{2} + \frac{\bar{\Theta}^2}{5}\right)\times(7.245\times10^7w^2 - 4.184\times10^8w + 8.136\times10^{10}) - 4\Lambda k^{-1}L^4\left(\frac{1}{5} - \frac{\bar{\Theta}}{3} + \frac{\bar{\Theta}^2}{7}\right)(3.457\times10^{14}w^2 - 4.160\times10^{15}w + 4.663\times10^{19}) + 2\Lambda^2k^{-2}L^5\left(\frac{1}{7} - \frac{\bar{\Theta}}{4} + \frac{\bar{\Theta}^2}{9}\right)(2.905\times10^{21}w^2 - 7.211\times10^{22}w + 4.513\times10^{28})\Bigg], \tag{6}$$

For a Gaussian beam, substituting $\Lambda = 2L/kW^2$ into Eq. (6), which is equivalent to

$$\sigma_{I,l}^2(L) \approx 0.388\times10^{-8}\pi^2\varepsilon^{-1/3}\frac{\chi_T}{w^2}\Bigg[4L^3\left(\frac{1}{3} - \frac{\bar{\Theta}}{2} + \frac{\bar{\Theta}^2}{5}\right)\times(7.245\times10^7w^2 - 4.184\times10^8w + 8.136\times10^{10}) - 8k^{-2}W^{-2}L^5\left(\frac{1}{5} - \frac{\bar{\Theta}}{3} + \frac{\bar{\Theta}^2}{7}\right)(3.457\times10^{14}w^2 - 4.160\times10^{15}w + 4.663\times10^{19}) + 8k^{-4}W^{-4}L^7\left(\frac{1}{7} - \frac{\bar{\Theta}}{4} + \frac{\bar{\Theta}^2}{9}\right)(2.905\times10^{21}w^2 - 7.211\times10^{22}w + 4.513\times10^{28})\Bigg], \tag{7}$$

here W is beam radius in free space at receiver.

3. Numerical calculation and analysis

In this paper, wavelength $\lambda = 0.417$ μm is chosen [29]. In this section the results are obtained by analytical formula (i.e., (Eqs. (5)–7)), which are valid in the weak turbulence regime.

Fig. 1 shows changes of radial component of scintillation index $\sigma_{I,r}^2(\mathbf{r}, L)$ versus off-axis distance for Gaussian-beam wave. It indicates this quantity physically describes the off-axis contribution to the scintillation index. From Fig. 1, at the fixed propagation distance, it is shown that radial component of scintillation index increases as the off-axis distance increases.

Fig. 2 is plotted by changes of the radial component of scintillation index for a Gaussian-beam wave with propagation distance $L$and three oceanic parameters (i.e. w, χ_T and ε) when

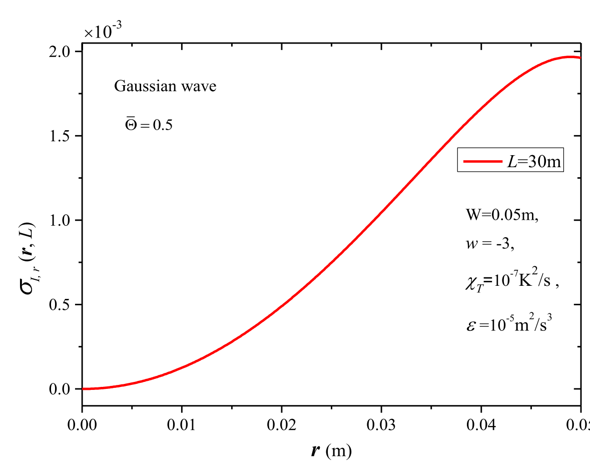

Fig. 1. Radial component of scintillation index as a function of r for a Gaussian-beam wave.

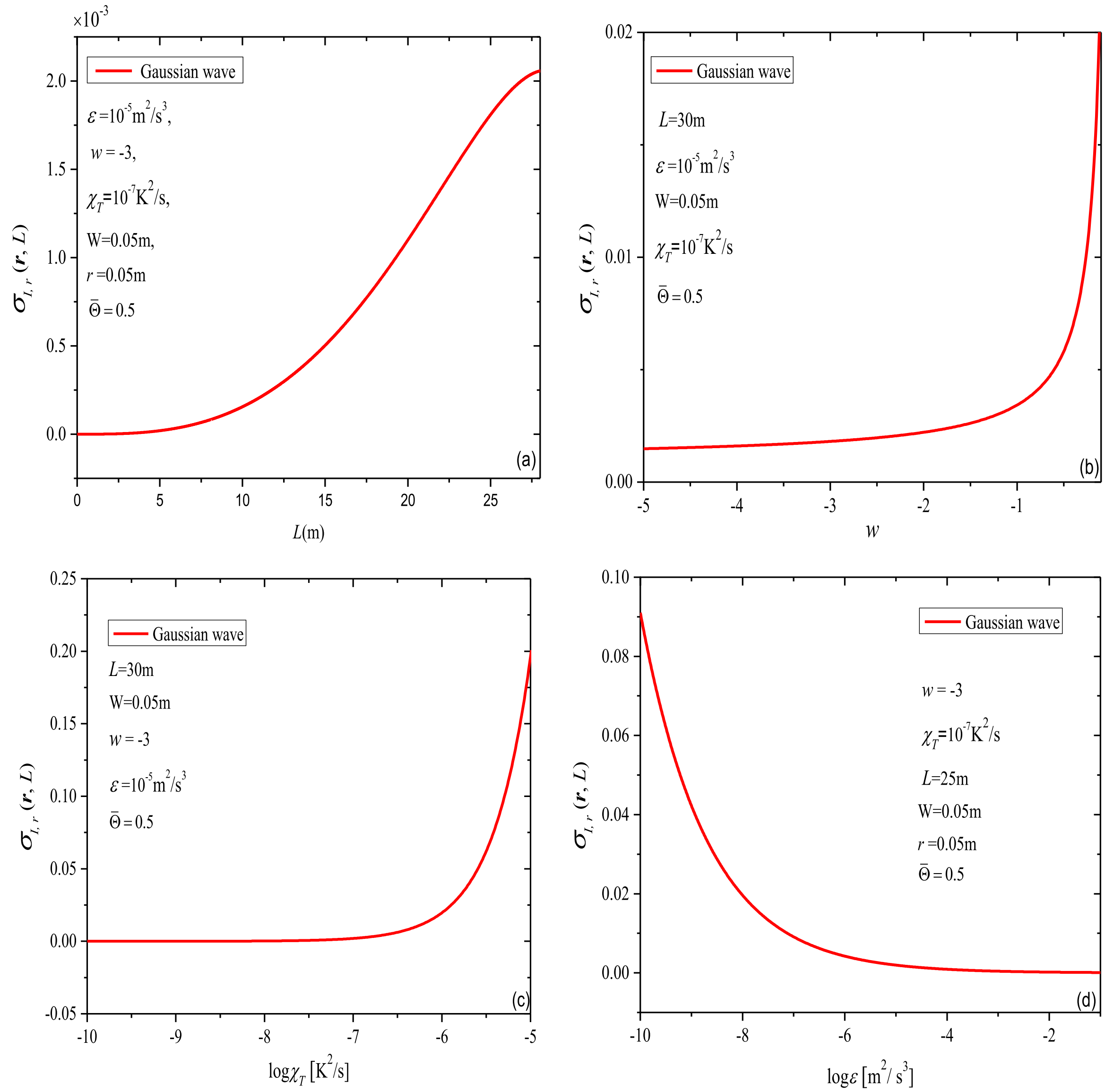

Fig. 2. Radial component of scintillation index for a Gaussian-beam wave as a function of (a) propagation distance L, (b) w, (c) log χ_T and (d) log ε.

$\bar{\Theta}$ = 0.5 is chosen. In Fig. 2(a), the radial component of scintillation increases as propagation distance increases. In Fig. 2(b), it is shown that $\sigma_{I,r}^2(\mathbf{r}, L)$ has larger value when oceanic turbulence is dominated by the salinity-induced. In Fig. 2(c), radial component of scintillation index $\sigma_{I,r}^2(\mathbf{r}, L)$ increases as χ_T increases. From Ref. [30], the higher values χ_T generally mean in regions of strongly stratified water and energetic turbulence. In our research, when χ_T attains a large value, the scintillation has a larger value. The more energetic turbulent strength yields the larger scintillations. In Fig. 2(d), we can obtain radial component of scintillation index $\sigma_{I,r}^2(\mathbf{r}, L)$ is inversely proportion to the rate of dissipation of the turbulent kinetic energy ε for the Gaussian wave.

In order to distinguish the difference between the analytical results (i.e., based on Eq. (6)) and the numerical results in Ref. [20], we give a comparison of results of $\sigma_{I,l}^2(\mathbf{r}, L)$ calculated by the analytical formula obtained in this paper and by Eq. (2) in Ref. [20]. Fig. 3 is plotted by comparing theoretical with analytical longitudinal components of scintillation index, as a function of propagation distance. It is shown that two results are in agreement with each other exactly at the fixed parameters. From Fig. 3, the longest turbulent distance increases as w decreases. Besides, to the longest weak turbulence distance for three wave models, the plane wave is the shortest and spherical wave is the longest.

From Fig. 4, we focus on longitudinal component of scintillation index for three kind of waves (i.e., plane, Gaussian and spherical waves) and analyze numerically under weak turbulence regime (i.e., $\sigma_{I,l}^2(\mathbf{r}, L) < 1$). Fig. 4(a) shows the longitudinal component of scintillation index versus the propagation distance $L$for plane, Gaussian and spherical waves with the same parameters. As expected, three models of scintillations increase as propagation distance increases. The longitudinal component of scintillations increase more drastically for plane wave than Gaussian and spherical waves, which indicates the plane wave is affected significantly at the fixed turbulent strength. The longest weak turbulence distance for a plane wave is shorter than that for a Gaussian or spherical wave. In Fig. 4(b), we can see that the salinity-induced turbulence increases the longitudinal component of scintillations much more than the temperature-induced turbulence for three kinds of waves. Similar to the results presented in Fig. 4(a), the plane wave tends to be affected significantly as compared to the others. The scintillations are higher for larger w values, i.e., when underwater turbulence is dominated by the salinity fluctuations. Fig. 4(c) shows longitudinal component of

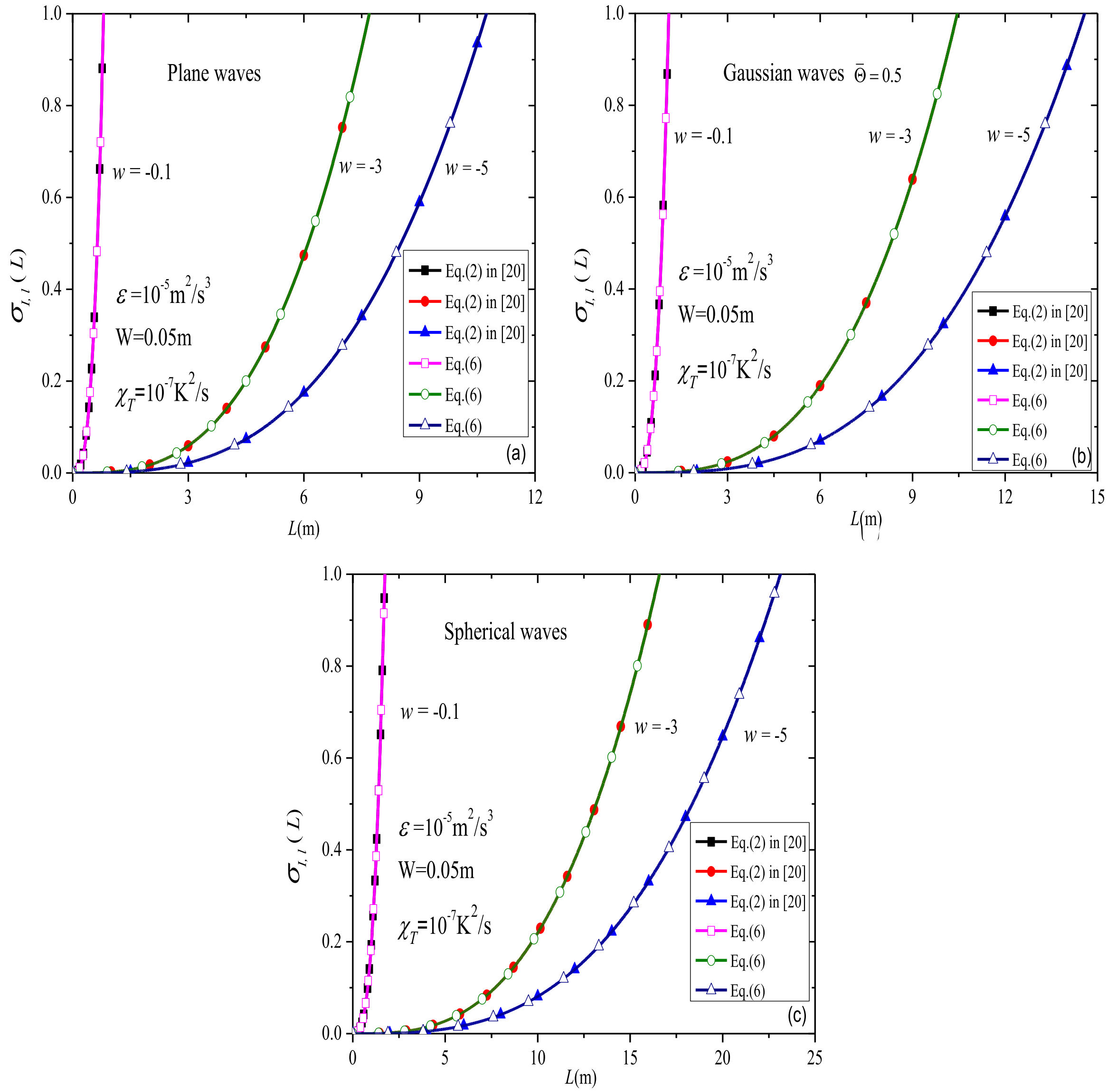

Fig. 3. Comparing theoretical with analytical longitudinal components of scintillation index as a function of propagation distance L for three wave models.

scintillation index versus with χ_T for plane, Gaussian-beam and spherical waves, respectively. As expected, large rates of dissipation of mean squared temperature yields large scintillations for three kinds of waves. Under the same turbulence parameters, the scintillations for the plane wave in seawater are largest and that of spherical one are smallest. Fig. 4(d) is plotted by changes of the longitudinal component of scintillation index with $\varepsilon$for the plane, Gaussian and spherical waves, respectively. It is shown that when the rate of dissipation of the turbulent kinetic energy increases, the scintillation decreases. Similar to the results presented in Fig. 4 (a)–(c), the plane wave tends to be affected the most significantly as compared to the rest of models.

4. Conclusions

In this paper, the analytical expressions of radial and longitudinal components of scintillation index are deduced under weak turbulence regime for the first time. The influences of radial component of scintillation index with the off-axis distance, propagation distance and three main oceanic parameters (i.e., the ratio of temperature to salinity contribution to the refractive index spectrum w, and the rate of dissipation of the mean squared temperature χ_T increase and the rate of dissipation of the turbulent kinetic energy ε) for Gaussian wave are investigated. The radial component of scintillation index for Gaussian wave is evaluated in oceanic turbulence. It is shown that the radial component of scintillation index increases as the off-axis distance r, propagation distance L, the ratio of temperature to salinity contribution to the refractive index spectrum w, and the rate of dissipation of the mean squared temperature χ_T increase while the radial component of scintillation index increases as the rate of dissipation of the turbulent kinetic energy εdecreases. Similar to radial component of scintillation index, the longitudinal component of scintillation index increases as propagation distance L, the relative strength of temperature and salinity$w$and the rate of dissipation of the mean squared temperature χ_T increase, and the rate of dissipation of the turbulent kinetic energy ε decreases. Besides, the longitudinal component of scintillations increases more drastically for plane wave than others, which indicates the plane wave is affected significantly at the fixed turbulent strength. The longest weak turbulence distance for a plane wave is shorter than that for a Gaussian or spherical wave. It's believed that this work can benefit to communication systems in seawater.

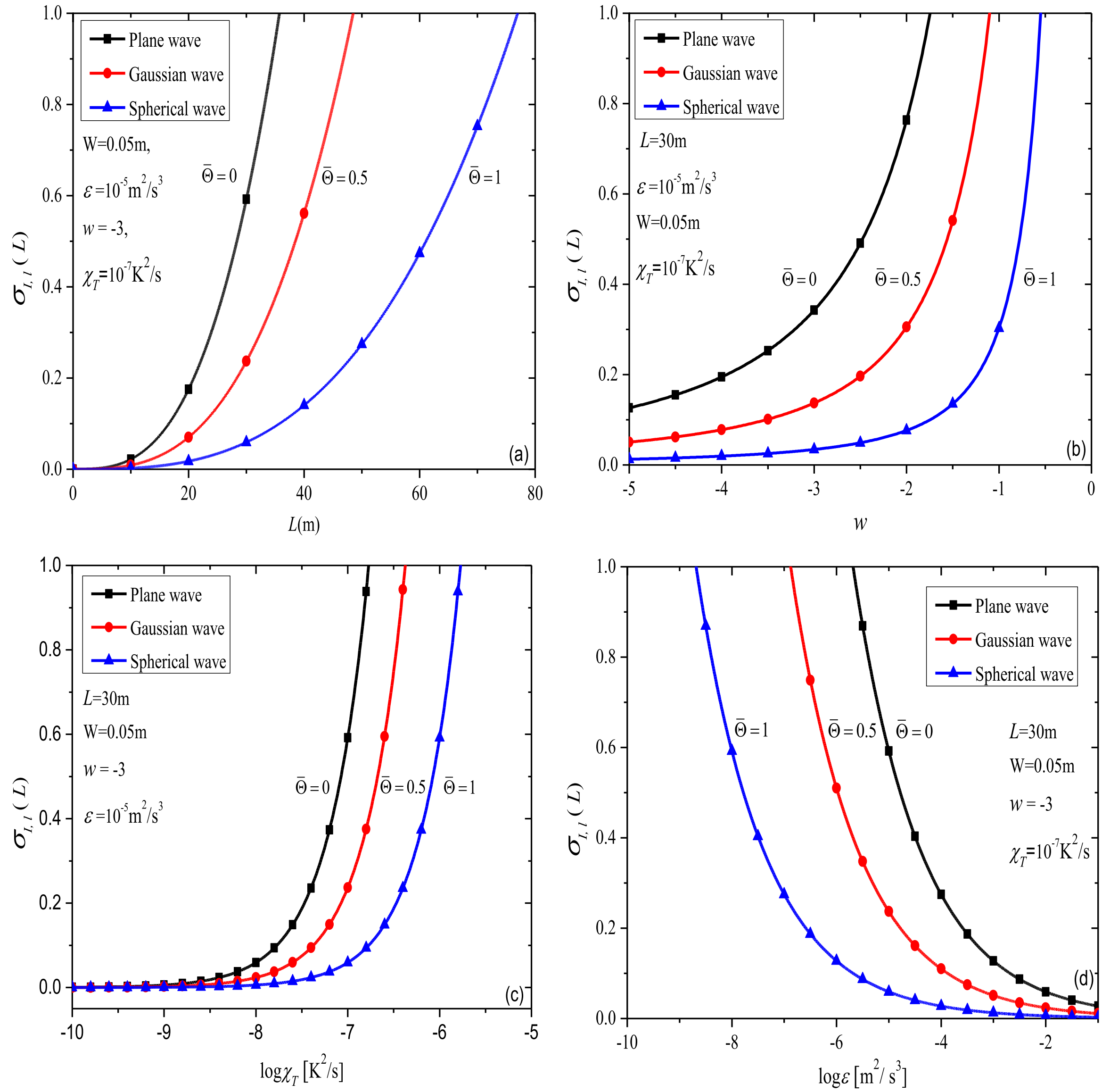

Fig. 4. Longitudinal component of scintillation index for three wave models as a function of (a) propagation distance L, (b) w, (c) log χ_T and (d) log ε.

Acknowledgments

Zhiqiang Wang, Pengfei Zhang, Chunhong Qiao, Lu Lu, Chengyu Fan and Xiaoling Ji acknowledge the support by the National Natural Science Foundation of China (NSFC) under Grant 61405205 and 61475105.

Appendix

Based on the property of modified Bessel function $I_0(2\Lambda r\xi\kappa) - 1 = \sum_{n=1}^{\infty}(\Lambda r)^{2n}k^{2n}\xi^{2n}/(n!)^2$, the radial component of scintillation index is expressed as

$$\sigma_{I,r}^2(\mathbf{r}, L) = 8\pi^2k^2L\int_0^1\int_0^\infty \kappa\Phi_n(\kappa)\exp\left(-\frac{\Lambda L\kappa^2\xi^2}{k}\right)\sum_{n=1}^{\infty}(\Lambda r)^{2n}k^{2n}\xi^{2n}/(n!)^2 d\kappa d\xi, \tag{8}$$

Interchanged the order of summation and integration, and substituting the integrals [31] into Eq. (8), the radial component of scintillation index can be expressed as

$$
\begin{aligned}
\sigma_{I,r}^2(\mathbf{r},L) \approx{}& 8\pi^2k^2L\times 0.388\times 10^{-8}\varepsilon^{-1/3}\frac{\chi_T}{w^2}\Bigg\{\frac{1}{2}\Gamma\left(-\frac{5}{6}\right)b^{\frac{5}{6}}w^2\left(1-\frac{7a^3}{216b^2}\right)\left[1-{}_2F_2\left(-\frac{5}{6},\frac{1}{2};1,\frac{3}{2};\frac{\Lambda^2r^2}{b}\right)\right]\\
&+\frac{1}{2}\Gamma\left(-\frac{5}{6}\right)d^{\frac{5}{6}}\left(1-\frac{7c^3}{216d^2}\right)\left[1-{}_2F_2\left(-\frac{5}{6},\frac{1}{2};1,\frac{3}{2};\frac{\Lambda^2r^2}{d}\right)\right]-\Gamma\left(-\frac{5}{6}\right)f^{\frac{5}{6}}w\left(1-\frac{7e^3}{216f^2}\right)\left[1-{}_2F_2\left(-\frac{5}{6},\frac{1}{2};1,\frac{3}{2};\frac{\Lambda^2r^2}{f}\right)\right]\\
&+\frac{5}{12}\Gamma\left(-\frac{5}{6}\right)ab^{-\frac{1}{6}}gw^2\left(1-\frac{91a^3}{864b^2}\right)\left[1-{}_2F_2\left(\frac{1}{6},\frac{1}{2};1,\frac{3}{2};\frac{\Lambda^2r^2}{b}\right)\right]\\
&+\frac{5}{12}\Gamma\left(-\frac{5}{6}\right)cd^{-\frac{1}{6}}g\left(1-\frac{91c^3}{864d^2}\right)\left[1-{}_2F_2\left(\frac{1}{6},\frac{1}{2};1,\frac{3}{2};\frac{\Lambda^2r^2}{d}\right)\right]\\
&-\frac{5}{6}\Gamma\left(-\frac{5}{6}\right)ef^{-\frac{1}{6}}gw\left(1-\frac{91e^3}{864f^2}\right)\left[1-{}_2F_2\left(\frac{1}{6},\frac{1}{2};1,\frac{3}{2};\frac{\Lambda^2r^2}{f}\right)\right]+\frac{1}{2}\Gamma\left(-\frac{1}{2}\right)b^{\frac{1}{2}}gw^2\left(1-\frac{a^3}{8b^2}\right)\left[1-{}_2F_2\left(-\frac{1}{2},\frac{1}{2};1,\frac{3}{2};\frac{\Lambda^2r^2}{b}\right)\right]\\
&+\frac{1}{2}\Gamma\left(-\frac{1}{2}\right)d^{\frac{1}{2}}g\left(1-\frac{c^3}{8d^2}\right)\left[1-{}_2F_2\left(-\frac{1}{2},\frac{1}{2};1,\frac{3}{2};\frac{\Lambda^2r^2}{d}\right)\right]-\Gamma\left(-\frac{1}{2}\right)f^{\frac{1}{2}}gw\left(1-\frac{e^3}{8f^2}\right)\left[1-{}_2F_2\left(-\frac{1}{2},\frac{1}{2};1,\frac{3}{2};\frac{\Lambda^2r^2}{f}\right)\right]\\
&-\frac{1}{8}\Gamma\left(-\frac{1}{2}\right)a^2b^{-\frac{1}{2}}w^2\left(1-\frac{a^3}{16b^2}\right)\left[1-{}_2F_2\left(\frac{1}{2},\frac{1}{2};1,\frac{3}{2};\frac{\Lambda^2r^2}{b}\right)\right]-\frac{1}{8}\Gamma\left(-\frac{1}{2}\right)c^2d^{-\frac{1}{2}}\left(1-\frac{c^3}{16d^2}\right)\left[1-{}_2F_2\left(\frac{1}{2},\frac{1}{2};1,\frac{3}{2};\frac{\Lambda^2r^2}{d}\right)\right]\\
&+\frac{1}{4}\Gamma\left(-\frac{1}{2}\right)e^2f^{-\frac{1}{2}}w\left(1-\frac{e^3}{16f^2}\right)\left[1-{}_2F_2\left(\frac{1}{2},\frac{1}{2};1,\frac{3}{2};\frac{\Lambda^2r^2}{f}\right)\right]\\
&-\frac{1}{2}\Gamma\left(-\frac{1}{6}\right)ab^{\frac{1}{6}}w^2\left(1-\frac{55a^3}{864b^2}\right)\left[1-{}_2F_2\left(-\frac{1}{6},\frac{1}{2};1,\frac{3}{2};\frac{\Lambda^2r^2}{b}\right)\right]\\
&-\frac{1}{2}\Gamma\left(-\frac{1}{6}\right)cd^{\frac{1}{6}}\left(1-\frac{55c^3}{864d^2}\right)\left[1-{}_2F_2\left(-\frac{1}{6},\frac{1}{2};1,\frac{3}{2};\frac{\Lambda^2r^2}{d}\right)\right]+\Gamma\left(-\frac{1}{6}\right)ef^{\frac{1}{6}}w\left(1-\frac{55e^3}{864f^2}\right)\left[1-{}_2F_2\left(-\frac{1}{6},\frac{1}{2};1,\frac{3}{2};\frac{\Lambda^2r^2}{f}\right)\right]\\
&-\frac{1}{24}\Gamma\left(-\frac{1}{6}\right)a^2b^{-\frac{5}{6}}gw^2\left(1-\frac{187a^3}{2160b^2}\right)\left[1-{}_2F_2\left(\frac{5}{6},\frac{1}{2};1,\frac{3}{2};\frac{\Lambda^2r^2}{b}\right)\right]\\
&-\frac{1}{24}\Gamma\left(-\frac{1}{6}\right)c^2d^{-\frac{5}{6}}g\left(1-\frac{187c^3}{2160d^2}\right)\left[1-{}_2F_2\left(\frac{5}{6},\frac{1}{2};1,\frac{3}{2};\frac{\Lambda^2r^2}{d}\right)\right]\\
&+\frac{1}{12}\Gamma\left(-\frac{1}{6}\right)e^2f^{-\frac{5}{6}}gw\left(1-\frac{187e^3}{2160f^2}\right)\left[1-{}_2F_2\left(\frac{5}{6},\frac{1}{2};1,\frac{3}{2};\frac{\Lambda^2r^2}{f}\right)\right]\Bigg\}\\
&-8\pi^2\times 0.388\times 10^{-8}W^{-2}L^3\varepsilon^{-1/3}\frac{\chi_T}{w^2}\Bigg\{\frac{1}{6}\Gamma\left(\frac{1}{6}\right)b^{-\frac{1}{6}}w^2\left(1-\frac{91a^3}{216b^2}\right)\left[1-{}_2F_2\left(\frac{1}{6},\frac{3}{2};1,\frac{5}{2};\frac{\Lambda^2r^2}{b}\right)\right]\\
&+\frac{1}{6}\Gamma\left(\frac{1}{6}\right)d^{-\frac{1}{6}}\left(1-\frac{91c^3}{216d^2}\right)\left[1-{}_2F_2\left(\frac{1}{6},\frac{3}{2};1,\frac{5}{2};\frac{\Lambda^2r^2}{d}\right)\right]-\frac{1}{3}\Gamma\left(\frac{1}{6}\right)f^{-\frac{1}{6}}w\left(1-\frac{91e^3}{216f^2}\right)\left[1-{}_2F_2\left(\frac{1}{6},\frac{3}{2};1,\frac{5}{2};\frac{\Lambda^2r^2}{f}\right)\right]\\
&-\frac{1}{36}\Gamma\left(\frac{1}{6}\right)ab^{-\frac{7}{6}}gw^2\left(1-\frac{247a^3}{432b^2}\right)\left[1-{}_2F_2\left(\frac{7}{6},\frac{3}{2};1,\frac{5}{2};\frac{\Lambda^2r^2}{b}\right)\right]-\frac{1}{36}\Gamma\left(\frac{1}{6}\right)cd^{-\frac{7}{6}}g\left(1-\frac{247c^3}{432d^2}\right)\left[1-{}_2F_2\left(\frac{7}{6},\frac{3}{2};1,\frac{5}{2};\frac{\Lambda^2r^2}{d}\right)\right]\\
&+\frac{1}{18}\Gamma\left(\frac{1}{6}\right)ef^{-\frac{7}{6}}gw\left(1-\frac{247e^3}{432f^2}\right)\left[1-{}_2F_2\left(\frac{7}{6},\frac{3}{2};1,\frac{5}{2};\frac{\Lambda^2r^2}{f}\right)\right]+\frac{1}{6}\Gamma\left(\frac{1}{2}\right)b^{-\frac{1}{2}}gw^2\left(1-\frac{a^3}{8b^2}\right)\left[1-{}_2F_2\left(\frac{1}{2},\frac{3}{2};1,\frac{5}{2};\frac{\Lambda^2r^2}{b}\right)\right]\\
&+\frac{1}{6}\Gamma\left(\frac{1}{2}\right)d^{-\frac{1}{2}}g\left(1-\frac{c^3}{8d^2}\right)\left[1-{}_2F_2\left(\frac{1}{2},\frac{3}{2};1,\frac{5}{2};\frac{\Lambda^2r^2}{d}\right)\right]-\frac{1}{3}\Gamma\left(\frac{1}{2}\right)f^{-\frac{1}{2}}gw\left(1-\frac{e^3}{8f^2}\right)\left[1-{}_2F_2\left(\frac{1}{2},\frac{3}{2};1,\frac{5}{2};\frac{\Lambda^2r^2}{f}\right)\right]\\
&+\frac{1}{24}\Gamma\left(\frac{1}{2}\right)a^2b^{-\frac{3}{2}}w^2\left(1-\frac{7a^3}{48b^2}\right)\left[1-{}_2F_2\left(\frac{3}{2},\frac{3}{2};1,\frac{5}{2};\frac{\Lambda^2r^2}{b}\right)\right]+\frac{1}{24}\Gamma\left(\frac{1}{2}\right)c^2d^{-\frac{3}{2}}\left(1-\frac{7c^3}{48d^2}\right)\left[1-{}_2F_2\left(\frac{3}{2},\frac{3}{2};1,\frac{5}{2};\frac{\Lambda^2r^2}{d}\right)\right]\\
&-\frac{1}{12}\Gamma\left(\frac{1}{2}\right)e^2f^{-\frac{3}{2}}w\left(1-\frac{7e^3}{48f^2}\right)\left[1-{}_2F_2\left(\frac{3}{2},\frac{3}{2};1,\frac{5}{2};\frac{\Lambda^2r^2}{f}\right)\right]-\frac{1}{6}\Gamma\left(\frac{5}{6}\right)ab^{-\frac{5}{6}}w^2\left(1-\frac{187a^3}{864b^2}\right)\left[1-{}_2F_2\left(\frac{5}{6},\frac{3}{2};1,\frac{5}{2};\frac{\Lambda^2r^2}{b}\right)\right]\\
&-\frac{1}{6}\Gamma\left(\frac{5}{6}\right)cd^{-\frac{5}{6}}\left(1-\frac{187c^3}{864d^2}\right)\left[1-{}_2F_2\left(\frac{5}{6},\frac{3}{2};1,\frac{5}{2};\frac{\Lambda^2r^2}{d}\right)\right]+\frac{1}{3}\Gamma\left(\frac{5}{6}\right)ef^{-\frac{5}{6}}w\left(1-\frac{187e^3}{864f^2}\right)\left[1-{}_2F_2\left(\frac{5}{6},\frac{3}{2};1,\frac{5}{2};\frac{\Lambda^2r^2}{f}\right)\right]\\
&+\frac{5}{72}\Gamma\left(\frac{5}{6}\right)a^2b^{-\frac{11}{6}}gw^2\left(1-\frac{391a^3}{432b^2}\right)\left[1-{}_2F_2\left(\frac{11}{6},\frac{3}{2};1,\frac{5}{2};\frac{\Lambda^2r^2}{b}\right)\right]\\
&+\frac{5}{72}\Gamma\left(\frac{5}{6}\right)c^2d^{-\frac{5}{6}}g\left(1-\frac{391c^3}{432d^2}\right)\left[1-{}_2F_2\left(\frac{11}{6},\frac{3}{2};1,\frac{5}{2};\frac{\Lambda^2r^2}{d}\right)\right]\\
&-\frac{5}{36}\Gamma\left(\frac{5}{6}\right)e^2f^{-\frac{11}{6}}gw\left(1-\frac{391e^3}{432f^2}\right)\left[1-{}_2F_2\left(\frac{11}{6},\frac{3}{2};1,\frac{5}{2};\frac{\Lambda^2r^2}{f}\right)\right]\Bigg\},
\end{aligned}
\tag{9}
$$

where $a = 8.284A_T\eta^{4/3}$, $b = 12.978A_T\eta^2$, $c = 8.284A_S\eta^{4/3}$, $d = 12.978A_S\eta^2$, $e = 8.284A_{TS}\eta^{4/3}$, $f = 12.978A_{TS}\eta^2$, $g = 2.35\eta^{2/3}$, r is off-axis distance and ${}_2F_2(a, b; c, d; x)$ is the confluent hypergeometric function (Appendix I in Ref. [28]).

Using the properties of confluent hypergeometric function in the Appendix in Ref. [28], it can be shown that radial component of scintillation index is given as

$$
\begin{aligned}
\sigma_{l,r}^{2}(\mathbf{r},L) \approx{} & 8\pi^2k^2L\times 0.388\times 10^{-8}\varepsilon^{-1/3}\frac{\chi_T}{w^2}\Bigg\{\frac{5}{36}\Gamma\left(-\frac{5}{6}\right)b^{\frac{5}{6}}w^2\left(1-\frac{7a^3}{216b^2}\right)\frac{\Lambda^2r^2}{b}\\
&+\frac{5}{36}\Gamma\left(-\frac{5}{6}\right)d^{\frac{5}{6}}\left(1-\frac{7c^3}{216d^2}\right)\frac{\Lambda^2r^2}{d}-\frac{5}{18}\Gamma\left(-\frac{5}{6}\right)f^{\frac{5}{6}}w\left(1-\frac{7e^3}{216f^2}\right)\frac{\Lambda^2r^2}{f}\\
&+\frac{5}{12}\Gamma\left(-\frac{5}{6}\right)ab^{-\frac{1}{6}}gw^2\left(1-\frac{91a^3}{864b^2}\right)\left(-\frac{\Lambda^2r^2}{18b}\right)+\frac{5}{12}\Gamma\left(-\frac{5}{6}\right)cd^{-\frac{1}{6}}g\left(1-\frac{91c^3}{864d^2}\right)\left(-\frac{\Lambda^2r^2}{18d}\right)\\
&-\frac{5}{6}\Gamma\left(-\frac{5}{6}\right)ef^{-\frac{1}{6}}gw\left(1-\frac{91e^3}{864f^2}\right)\left(-\frac{\Lambda^2r^2}{18f}\right)+\frac{1}{2}\Gamma\left(-\frac{1}{2}\right)b^{\frac{1}{2}}gw^2\left(1-\frac{a^3}{8b^2}\right)\frac{\Lambda^2r^2}{6b}\\
&+\frac{1}{2}\Gamma\left(-\frac{1}{2}\right)d^{\frac{1}{2}}g\left(1-\frac{c^3}{8d^2}\right)\frac{\Lambda^2r^2}{6d}-\Gamma\left(-\frac{1}{2}\right)f^{\frac{1}{2}}gw\left(1-\frac{e^3}{8f^2}\right)\frac{\Lambda^2r^2}{6f}\\
&\qquad-\frac{1}{8}\Gamma\left(-\frac{1}{2}\right)a^2b^{-\frac{1}{2}}w^2\left(1-\frac{a^3}{16b^2}\right)\left(-\frac{\Lambda^2r^2}{6b}\right)-\frac{1}{8}\Gamma\left(-\frac{1}{2}\right)c^2d^{-\frac{1}{2}}\left(1-\frac{c^3}{16d^2}\right)\left(-\frac{\Lambda^2r^2}{6d}\right)\\
&+\frac{1}{4}\Gamma\left(-\frac{1}{2}\right)e^2f^{-\frac{1}{2}}w\left(1-\frac{e^3}{16f^2}\right)\left(-\frac{\Lambda^2r^2}{6f}\right)-\frac{1}{2}\Gamma\left(-\frac{1}{6}\right)ab^{\frac{1}{6}}w^2\left(1-\frac{55a^3}{864b^2}\right)\frac{\Lambda^2r^2}{18b}\\
&-\frac{1}{2}\Gamma\left(-\frac{1}{6}\right)cd^{\frac{1}{6}}\left(1-\frac{55c^3}{864d^2}\right)\frac{\Lambda^2r^2}{18d}+\Gamma\left(-\frac{1}{6}\right)ef^{\frac{1}{6}}w\left(1-\frac{55e^3}{864f^2}\right)\frac{\Lambda^2r^2}{18f}\\
&-\frac{1}{24}\Gamma\left(-\frac{1}{6}\right)a^2b^{-\frac{5}{6}}gw^2\left(1-\frac{187a^3}{2160b^2}\right)\left(-\frac{5\Lambda^2r^2}{18b}\right)-\frac{1}{24}\Gamma\left(-\frac{1}{6}\right)c^2d^{-\frac{5}{6}}g\left(1-\frac{187c^3}{2160d^2}\right)\left(-\frac{5\Lambda^2r^2}{18d}\right)\\
&+\frac{1}{12}\Gamma\left(-\frac{1}{6}\right)e^2f^{-\frac{5}{6}}gw\left(1-\frac{187e^3}{2160f^2}\right)\left(-\frac{5\Lambda^2r^2}{18f}\right)\Bigg\}\\
&-8\pi^2\times 0.388\times 10^{-8}W^{-2}L^3\varepsilon^{-1/3}\frac{\chi_T}{w^2}\Bigg\{\frac{1}{6}\Gamma\left(\frac{1}{6}\right)b^{-\frac{1}{6}}w^2\left(1-\frac{91a^3}{216b^2}\right)\left(-\frac{\Lambda^2r^2}{10b}\right)\\
&+\frac{1}{6}\Gamma\left(\frac{1}{6}\right)d^{-\frac{1}{6}}\left(1-\frac{91c^3}{216d^2}\right)\left(-\frac{\Lambda^2r^2}{10d}\right)-\frac{1}{3}\Gamma\left(\frac{1}{6}\right)f^{-\frac{1}{6}}w\left(1-\frac{91e^3}{216f^2}\right)\left(-\frac{\Lambda^2r^2}{10f}\right)\\
&-\frac{1}{36}\Gamma\left(\frac{1}{6}\right)ab^{-\frac{7}{6}}gw^2\left(1-\frac{247a^3}{432b^2}\right)\left(-\frac{7\Lambda^2r^2}{10b}\right)-\frac{1}{36}\Gamma\left(\frac{1}{6}\right)cd^{-\frac{7}{6}}g\left(1-\frac{247c^3}{432d^2}\right)\left(-\frac{7\Lambda^2r^2}{10d}\right)\\
&+\frac{1}{18}\Gamma\left(\frac{1}{6}\right)ef^{-\frac{7}{6}}gw\left(1-\frac{247e^3}{432f^2}\right)\left(-\frac{7\Lambda^2r^2}{10f}\right)+\frac{1}{6}\Gamma\left(\frac{1}{2}\right)b^{-\frac{1}{2}}gw^2\left(1-\frac{a^3}{8b^2}\right)\left(-\frac{3\Lambda^2r^2}{10b}\right)\\
&+\frac{1}{6}\Gamma\left(\frac{1}{2}\right)d^{-\frac{1}{2}}g\left(1-\frac{c^3}{8d^2}\right)\left(-\frac{3\Lambda^2r^2}{10d}\right)-\frac{1}{3}\Gamma\left(\frac{1}{2}\right)f^{-\frac{1}{2}}gw\left(1-\frac{e^3}{8f^2}\right)\left(-\frac{3\Lambda^2r^2}{10f}\right)\\
&+\frac{1}{24}\Gamma\left(\frac{1}{2}\right)a^2b^{-\frac{3}{2}}w^2\left(1-\frac{7a^3}{48b^2}\right)1\left(-\frac{9\Lambda^2r^2}{10b}\right)+\frac{1}{24}\Gamma\left(\frac{1}{2}\right)c^2d^{-\frac{3}{2}}\left(1-\frac{7c^3}{48d^2}\right)\left(-\frac{9\Lambda^2r^2}{10d}\right)\\
&-\frac{1}{12}\Gamma\left(\frac{1}{2}\right)e^2f^{-\frac{3}{2}}w\left(1-\frac{7e^3}{48f^2}\right)\left(-\frac{9\Lambda^2r^2}{10f}\right)-\frac{1}{6}\Gamma\left(\frac{5}{6}\right)ab^{-\frac{5}{6}}w^2\left(1-\frac{187a^3}{864b^2}\right)\left(-\frac{\Lambda^2r^2}{2b}\right)\\
&-\frac{1}{6}\Gamma\left(\frac{5}{6}\right)cd^{-\frac{5}{6}}\left(1-\frac{187c^3}{864d^2}\right)\left(-\frac{\Lambda^2r^2}{2d}\right)+\frac{1}{3}\Gamma\left(\frac{5}{6}\right)ef^{-\frac{5}{6}}w\left(1-\frac{187e^3}{864f^2}\right)\left(-\frac{\Lambda^2r^2}{2f}\right)\\
&+\frac{5}{72}\Gamma\left(\frac{5}{6}\right)a^2b^{-\frac{11}{6}}gw^2\left(1-\frac{391a^3}{432b^2}\right)\left(-\frac{11\Lambda^2r^2}{10b}\right)+\frac{5}{72}\Gamma\left(\frac{5}{6}\right)c^2d^{-\frac{5}{6}}g\left(1-\frac{391c^3}{432d^2}\right)\left(-\frac{11\Lambda^2r^2}{10d}\right)\\
&-\frac{5}{36}\Gamma\left(\frac{5}{6}\right)e^2f^{-\frac{11}{6}}gw\left(1-\frac{391e^3}{432f^2}\right)\left(-\frac{11\Lambda^2r^2}{10f}\right)\Bigg\},
\end{aligned}
\tag{10}
$$

and substituting the fixed parameters in this paper, the analytical expression of radial component of scintillation index can be obtained as Eq. (5).

However, the analytical expression of longitudinal component of scintillation index component of scintillation index can be obtained by the same method in Ref. [32], after tedious calculation, the longitudinal component of scintillation index is expressed as Eq. (6) in this paper.

References

[1] A. Ishimaru, Wave Propagation and Scattering in Random Media, vol. 2, Academic, 1978.
[2] L.C. Andrews, R.L. Phillips, C.Y. Hopen, Laser Beam Scintillation with Applications, SPIE, 2001.
[3] H.T. Eyyuboğlu, Y. Baykal, Scintillation characteristics of cosh-Gaussian beams, Appl. Opt. 46 (2007) 1099–1106.
[4] S.A. Arpali, H.T. Eyyuboğlu, Y. Baykal, Scintillation index of higher-order cos-Gaussian, cosh-Gaussian and annular beams, J. Mod. Opt. 55 (2008) 227–239.
[5] Yangjian Cai, Halil T. Eyyuboğlu, Yahya Baykal, Scintillation of astigmatic dark hollow beams in weak atmospheric turbulence, J. Opt. Soc. Am. A 25 (7) (2008) 1497–1503.
[6] Min Yao, Scintillation index of astigmatic annular beams in a turbulent atmosphere, Optik 120 (2009) 824–828.
[7] Yangjian Cai, Yuntian Chen, Halil T. Eyyuboğlu, Yahya Baykal, Scintillation index of elliptical Gaussian beam in turbulent atmosphere, Opt. Lett. 32 (16) (2007) 2405–2407.
[8] H.T. Eyyuboğlu, Y. Baykal, X. Ji, Scintillations of laguerre gaussian beams, Appl. Phys. B 98 (2010) 857–863.
[9] y chen, y cai, ht eyyuboğlu, y baykal, Scintillation properties of dark hollow beams in a weak turbulent atmosphere, Appl. Phys. B 90 (2008) 87–92.
[10] Yahya Baykal, Halil T. Eyyuboğlu, Yangjian Cai, Effect of beam types on the scintillations: a review, in: Proceedings of SPIE, vol. 7200, 2009.
[11] Liying Tan, Wenhe Du, Jing Ma, Siyuan Yu, Qiqi Han, Log-amplitude variance for a Gaussian-beam wave propagating through non-Kolmogorov turbulence, Opt. Express 18 (2) (2010) 451–462.
[12] Yahya Baykal, Cross beam scintillations in non-Kolmogorov medium, J. Opt. Soc. Am. A 31 (10) (2014) 2198–2202.
[13] Yahya Baykal, Scintillations of higher-order laser beams in non-Kolmogorov medium, Opt. Lett. 39 (7) (2014) 2160–2163.
[14] Zhihong Zeng, Xiujuan Luo, Aili Xia, Yu Zhang, Bei Cao, Inner scale effect on scintillation index of flat-topped beam in non-Kolmogorov weak turbulence, Appl. Opt. 54 (10) (2015) 2630–2638.
[15] Avner Peleg, Jerome V. Moloney, Scintillation index for two Gaussian laser beams with different wavelengths in weak atmospheric turbulence, J. Opt. Soc. Am. A 23 (12) (2006) 3114–3122.
[16] Hamza Gerçekcioğlu, Yahya Baykal, Cem Nakiboğlu, Annular beam scintillations in strong turbulence, J. Opt. Soc. Am. A 27 (8) (2010) 1834–1839.
[17] Peng Deng, Xiu-Hua Yuan, Dexiu Huang, Scintillation of a laser beam propagation through non-Kolmogorov strong turbulence, Opt. Commun. 285 (2012) 880–887.
[18] R.J. Hill, Optical propagation in turbulent water, J. Opt. Soc. Am. 68 (1978) 1067–1072.
[19] O. Korotkova, N. Farwell, E. Shchepakina, Light scintillation in oceanic turbulence, Waves Random Complex Media 22 (2012) 260–266.
[20] Y. Ata, Y. Baykal, Scintillations of optical plane and spherical waves in underwater turbulence, J. Opt. Soc. Am. A 31 (7) (2014) 1552–1556.
[21] Masoud Yousefi, Shole Golmohammady, Ahmad Mashal, Fatemeh Dabbagh Kashahi, Analyzing the propagation behavior of scintillation index and bit error rate of a partially coherent flat-topped laser beam in oceanic turbulence, J. Opt. Soc. Am. A **32** (11) (2015) 1982–1991.
[22] Yahya Baykal, Intensity fluctuations of multimode laser beams in underwater medium, J. Opt. Soc. Am. A 32 (4) (2015) 593–598.
[23] Yahya Baykal, Higher order mode laser beam scintillations in oceanic medium, Waves in Random and Complex Media 26 (1) (2016) 21–29.
[24] Yahya Baykal, Higher-order laser beam scintillation in weakly turbulent marine atmospheric medium, J. Opt. Soc. Am. A 33 (4) (2016) 758–763.
[25] Yahya Baykal, Scintillation index in strong oceanic turbulence, Opt. Commun. 375 (2016) 15–18.
[26] V.V. Nikishov, V.I. Nikishov, Spectrum of turbulent fluctuations of the sea-water refraction index, Int. J. Fluid Mech. Res. 27 (2000) 82–98.
[27] N. Farwell, O. Kortkova, Intensity and coherence properties of light in oceanic turbulence, Opt. Commun. 285 (2012) 872.
[28] L.C. Andrews, R.L. Phillips, Laser Beam Propagation through Random Media, SPIE, 2005.
[29] M.P. Robin, S.F. Edward, Absorption spectrum 380–700 nm of pure water. II. Integrating cavity measurements, Appl. Opt. 36 (1997) 8710–8723.
[30] S.A. Thorpe, An Introduction to Turbulent Ocean, Cambridge University, United Kingdom, 2007.
[31] L. Lu, X.L. Ji, Y. Baykal, Wave structure function and spatial coherence radius of plane and spherical waves in oceanic turbulence, Opt. Express **22** (2014) 27112–27122.
[32] Lu Lu, Zhiqiang Wang, Pengfei Zhang, Chunhong Qiao, Chengyu Fan, Jinghui Zhang, Ji Xiaoling, Phase structure function and AOA Fluctuations of plane and spherical waves propagating through oceanic turbulence, J. Opt. 17 (2015) 085610.